Colloid Polym Sci (2009) 287:615–620
DOI 10.1007/s00396-009-2016-1

SHORT COMMUNICATION

# Crystallization and morphology of iPP/MWCNT prepared by compounding iPP melt with MWCNT aqueous suspension

**Chao-Lu Yin · Zheng-Ying Liu · Wei Yang · Ming-Bo Yang · Jian-Min Feng**

Received: 17 December 2008 / Revised: 7 February 2009 / Accepted: 9 February 2009 / Published online: 4 March 2009


**Abstract** In this work, isotactic polypropylene (iPP) composites filled with multiwalled carbon nanotubes (MWCNTs) were prepared by compounding iPP melt with MWCNT aqueous suspension using a corotating twin-screw extruder, and the morphology and crystallization behavior of the composites were investigated. Scanning electron microscopy micrographs showed that MWCNTs dispersed individually at nanoscale in the iPP matrix when the MWCNTs concentration was low, though MWCNTs aggregates were detected when the filler concentration increased. The results of differential scanning calorimetry, wide-angle X-ray diffraction, and polarized light microscopy indicated that the β-form crystal of iPP was induced by MWCNTs at the concentration of 0.1 wt.% which was dispersed individually in the iPP matrix. At higher content, however, MWCNTs acted as α-nucleating agent, and the crystals in the iPP/MWCNT composites showed higher degree of perfection than that of pure iPP though smaller in dimension. Crystallization rate of iPP increased significantly with increasing MWCNT content.

**Keywords** Isotactic polypropylene · MWCNTs · Aqueous suspension dispersion · Crystallization · β-crystal

## Introduction

Isotactic polypropylene (iPP)-based composites containing carbon nanotubes (CNTs), including single-walled CNTs (SWCNTs) and multiwalled CNTs (MWCNTs), have stimulated much interest due to their unusual properties, such as high mechanical strength, high thermal stability, and electronic conductivity. Reinforcement at nanoscale to improve mechanical and other properties including changes in PP crystallization behavior is being attempted [1, 2]. There have been extensive studies regarding crystallization behaviors of iPP in the presence of CNTs [3–8], as the crystallization behavior would have an important influence on the physical properties of the filled iPP. Most of these studies focused on the crystal forms of iPP [3, 4] or nucleating ability of CNTs for iPP crystallization [5]. Grady et al. [3] observed that octadecylamide-functionalized SWCNT promoted the formation of β-form iPP. In contrast, some other studies showed that SWCNTs [4] and MWCNTs [5, 7, 9] only promoted the formation of α-form iPP. Studies [5] showed that the composites exhibited fibrillar crystal rather than spherulitic crystal when MWCNT were introduced into iPP. The viewpoint that addition of MWCNTs increased the crystallization temperature and crystallization rate of polypropylene due to the heterogeneous nucleation effect of MWCNTs had been accepted by many researchers [4, 7, 10–12]. However, to the best of our knowledge, the effect of MWCNTs dispersion on the crystallization behavior of the iPP matrix have not been studied systemically and there are no reports of formation of β-form crystal in the iPP induced by MWCNTs without surface treatments to date.

It is well-known that the properties of polymer-based nanocomposites are strongly dependent on the dispersion of nanofillers. CNTs tend to aggregate to form bundles because of strong Van der Waal's force, which makes the dispersion of CNTs in the polymer matrix difficult. Extensive efforts have been devoted to study the effect of CNTs dispersion on the properties of the polymer matrix. Many manufacturing methods had been used to disperse CNTs in the polymer matrix, such as melt compounding CNTs with polymer, mixing CNTs in polymer solution, and

C.-L. Yin · Z.-Y. Liu · W. Yang · M.-B. Yang (✉) · J.-M. Feng
College of Polymer Science and Engineering,
State Key Laboratory of Polymer Materials Engineering,
Sichuan University,
Chengdu 610065 Sichuan, People's Republic of China
e-mail: yangmb@scu.edu.cn

in situ polymerization of polymer monomer with CNTs. Among all these methods, melt compounding has been regarded as a prevalent means for reasons of economy, convenience, practicability, and environment friendliness. However, the dispersion CNTs in the polymer matrix through melt compounding was not perfect due to strong aggregation of CNTs and poor compatibility between CNTs and polymer matrix. Consequently, techniques such as end-group chemical functionalization on the CNTs [3, 13–15] and modification by grafting reactive groups on the polymer matrix [16, 17] have been used to improve the dispersion of CNTs in the polymer matrix. The method of introduction of nanoparticle aqueous suspension into the polymer melt to prepare the nanocomposite in true physical meaning with fillers dispersing at nanoscale has been investigated in our group [18, 19], and the nanoparticles, such as $CaCO_3$ and carbon black, were dispersed quite well in thermoplastic polymer matrices. We are now attempting to apply this method to fabricate iPP/MWCNT nanocomposites.

In this work, the novel approach, compounding iPP melt with MWCNT aqueous suspension through twin-screw extruder, has been used to manufacture the iPP/MWCNT composites. The dispersion state of MWCNTs in the composites and the effect of MWCNTs on the crystallization behavior of the iPP matrix were investigated by means of scanning electron microscopy (SEM), differential scanning calorimetry (DSC), wide-angle X-ray diffraction (WAXD), and polarized light microscopy (PLM).

## Experimental

### Materials

A commercially available iPP (F401, Lanzhou Petroleum, China) with MFR=2.5 g/10 min was used as the matrix. The raw MWCNT, which possessed a diameter of about 10–20 nm, length of about 10–30 μm, and purity of more than 95%, was supplied by Chengdu Organic Chemistry, Chinese Academy of Sciences and used without any chemical treatment.

### Preparation of PP/MWCNT nanocomposites

The novel approach was used to manufacture the iPP/MWCNT composites. MWCNTs were first dispersed at nanoscale in aqueous suspension through a VCF-1500 ultrasonic irradiation instrument (Sonic & Materials, USA). Dispersing medium, hydoxyl-propyl-methyl cellulose (HPMC), was introduced into the aqueous suspension with a concentration of 0.005 g/mL to maintain the dispersion state of the nanoparticles in the suspension. MWCNT suspension was pumped into the cylinder at the second inlet on the corotating twin-screw extruder. The suspending liquid of the suspension was vaporized when contacting with the iPP melt, and at the same time, the MWCNTs were fed into the iPP matrix almost in the same state as they were in the suspension. The vapor of the suspending liquid, including the water-soluble material, mainly the HPMC, was expelled from the vent. The schematic diagram of the extrusion was shown in Fig. 1. In the compounding process, the feeding speed of iPP and pumping speed of MWCNTs aqueous suspension was kept constant, and the content of MWCNTs in the composites was controlled by adjusting the concentration of MWCNT aqueous suspension. The MWCNT aqueous suspensions were prepared at four different MWCNTs concentrations of 0.2, 1, 2, and 6 g/100 mL, and the corresponding MWCNT contents in the composites were 0.1, 0.5, 1, and 3 wt.%, respectively. The extruded samples were then pelletized. The pellets were dried at 80 °C for 3 h, and then injection molded into standard rectangular bars and dumbbell-shaped specimen using a PS40E5ASE injection molding machine, and the temperature was chosen as 190/210/230/225 °C from hopper to die.

### Characterizations

#### *Scanning electron microscopy*

To investigate the dispersion of MWCNTs in the iPP matrix, a FEI Inspect F SEM instrument was used to observe the fracture surface of the PP/MWCNT composites.

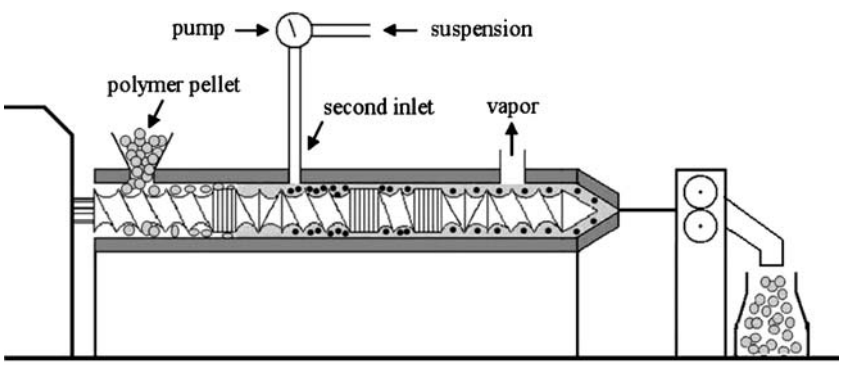


**Fig. 1** Schematic diagram of the extrusion using MWCNT aqueous suspension

The extruded samples were fractured in liquid nitrogen after about 0.5 h immersion. The fracture surfaces were gold coated and observed at an accelerating voltage of 10 KV.

*Differential scanning calorimetry*

Nonisothermal crystallization behaviors of the samples were determined using a TA Instruments' DSC Q20. The mass of the sample was about 5 mg. For nonisothermal crystallization, the sample was first heated to 200 °C, holding for 5 min to erase any previous thermal history, and then cooled to 80 °C with a scan rate of −10 K/min and then heated to 200 °C at a scan rate of 10 K/min. All DSC measurements were carried out under nitrogen atmosphere.

*Wide-angle X-ray diffraction*

WAXD analysis of the injection molded sample was conducted using a D/max-rA X-ray diffractometer. Graphite monochromatic Cu-Kα radiation was employed as a radiation source. The diffraction patterns of the samples were obtained at room temperature within the scanning range 3–50° using a scanning rate of 3°/min, a step length of 0.02°, a filament intensity of 110 mA, and an accelerating voltage of 42 KV.

*Polarized light microscopy*

Morphological observation of the iPP crystals were performed on a Leica DMIP polarized light microscopy equipped with a Linkam THMS 600 hot stage under crossed polarizers. The extruded samples were inserted between two microscopic cover glasses, melted at 200 °C, and squeezed to obtain thin films. The slices were held at 200 °C for 2 min on the stage to achieve thermal equilibrium. Subsequently, the melted slices were cooled down to room temperature with a rate of −3 K/min, and then in situ observations of the growth of the crystallites were implemented during the nonisothermal process.

## Results and discussion

Dispersion of MWCNT

Figure 2 shows the SEM micrographs of iPP/MWCNT composites with four MWCNT contents. From these micrographs, it can be seen that composites with different MWCNTs contents exhibited different MWCNT dispersion state. At low MWCNT content, most of the MWCNTs dispersed individually in the iPP matrix, as the SEM

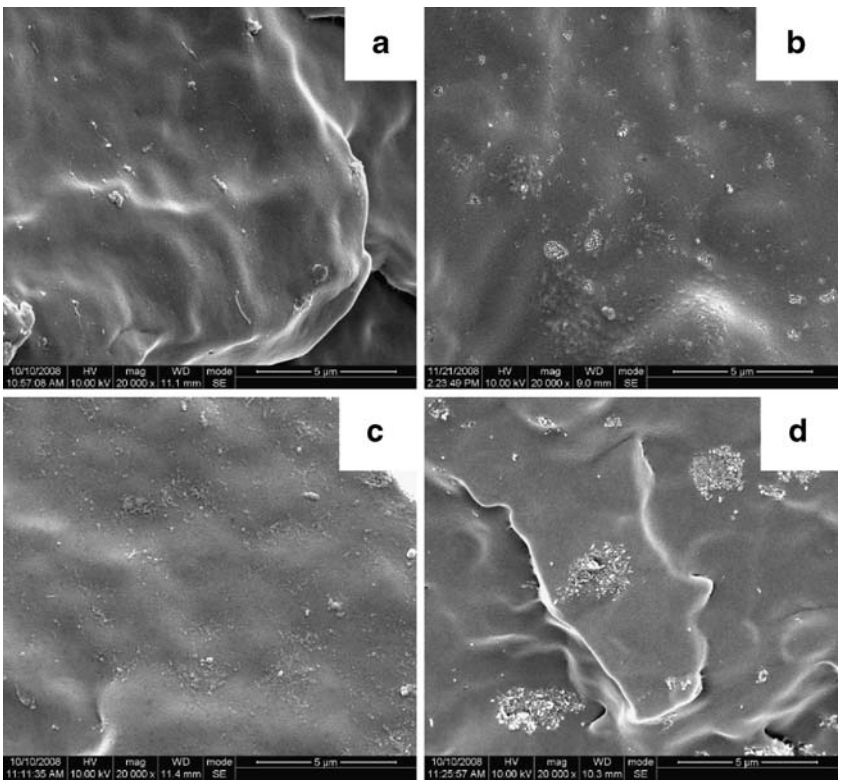


**Fig. 2** SEM micrographs of iPP/MWCNT composites. The content of MWCNT is 0.1 wt.% (**a**), 0.5 wt.% (**b**), 1 wt.% (**c**), and 3 wt.% (**d**), respectively

photograph of iPP/MWCNT composite with 0.1 wt.% MWCNTs showed (Fig. 2a). At relatively high MWCNT contents, MWCNT aggregates appeared in the polymer matrix, and the size of the aggregates increased with increasing MWCNTs content (showed as Fig. 2b–d). The uneven dispersion of MWCNTs at different MWCNT contents was partly due to the variation of MWCNT dispersion in aqueous suspension and suspension stability which was strongly dependent on the MWCNT concentration of the aqueous suspension [20, 21].

## DSC measurements

The effects of the contents and dispersion state of MWCNTs on the crystallization behavior of iPP were analyzed using DSC measurements. Figure 3a shows the nonisothermal crystallization curves of pure iPP and iPP/MWCNT composites with various MWCNT contents.

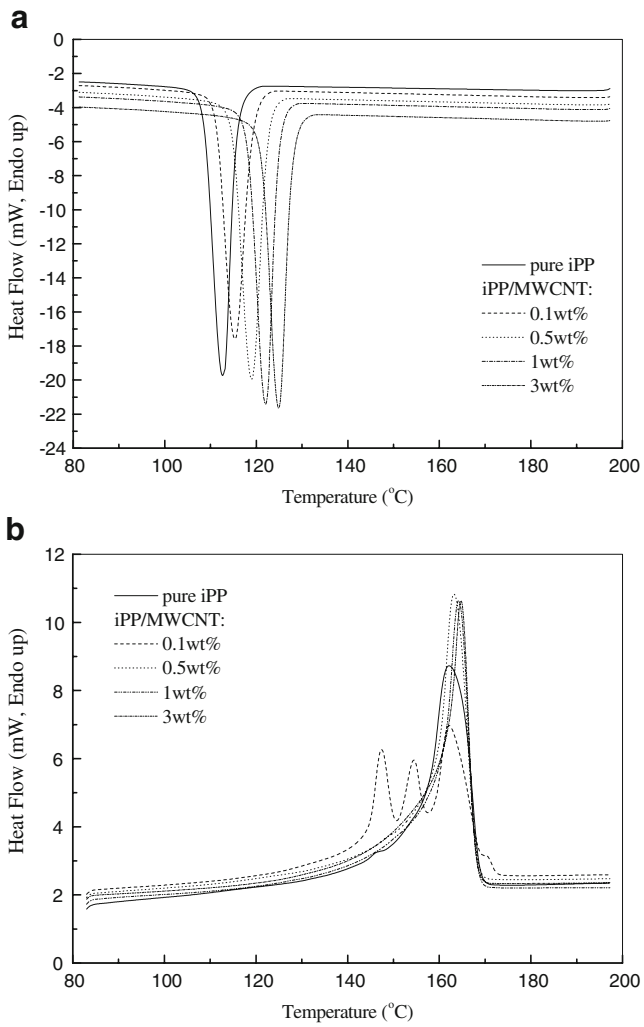


**Fig. 3** Nonisothermal crystallization (**a**) and melting (**b**) curves of pure iPP and iPP/MWCNT composites: pure iPP, 0.1 wt.%, 0.5 wt.%, 1 wt.%, and 3 wt.%

Obviously, the crystallization temperature increased with increasing of MWCNTs content gradually and an obvious increase of approximately 12 K was obtained when the MWCNT concentration reached 3 wt.%. It indicated that the MWCNTs acted as effective nucleating agents which were responsible for faster crystal growth in the iPP matrix. Similar results had been reported by many groups [7, 10–12].

The DSC melting curves of pure iPP and iPP/MWCNT composites after nonisothermal crystallization were shown in Fig. 3b. Two obvious peaks at approximately 147 and 154 °C appeared in the melting curve of the iPP/MWCNT composite with a MWCNT concentration of 0.1 wt.%. Polypropylene in the β-crystal form melts at lower temperature than the α-crystals, so the appearance of peak in the 147 and 154 °C temperature can be attributed to the melting of β-crystals or smaller or imperfect α-crystals. As will be discussed later, WAXD of the iPP/MWCNT composite with MWCNT content of 0.1% confirmed the presence of β-crystals. Considering that the pure iPP was not able to form the β-structure crystal under identical crystallization condition, it can be concluded that the presence of MWCNTs induced the growth of the β-form crystals in iPP. This result was surprising, since most studies [5, 7, 9, 10] suggested that MWCNTs could only promote the formation of α-iPP crystals, and no literature reported that MWCNTs could induce the formation of β-phase iPP. What should be pointed out was that the β-iPP crystals only appeared in the iPP/MWCNT composite with a low MWCNT content, although a series of iPP/MWCNT composites with various MWCNT content had been prepared. Similar results was reported by Medellín-Rodríguez and they proposed that, in the case of individual exfoliated layers of low nanoclay concentrations, the crystallographic requirements were satisfied to give nucleation and formation of the β-structure [22]. The dispersion states of MWCNT in the polypropylene matrix shown in the SEM micrograph,

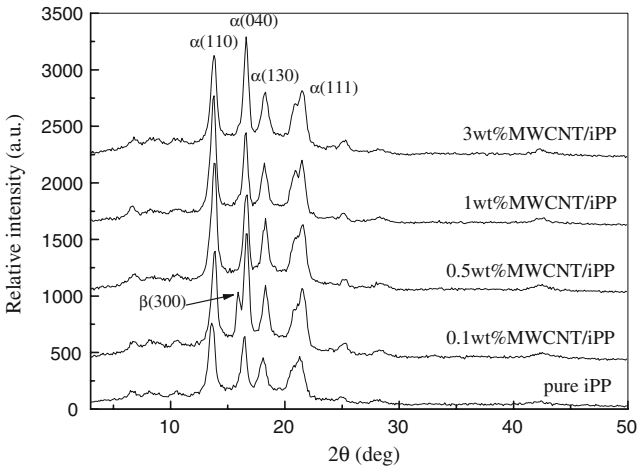


**Fig. 4** WAXRD patterns of pure iPP and iPP/MWCNT composites

together with the fact of the presence of the β-form crystals in the melting process, indicated that the MWCNTs could induce the formation of β-crystal form at low filler concentration. It was suggested that some of MWCNTs dispersed individually at nanoscale in the matrix at a low MWCNT content and these individual MWCNTs may served as β-nucleating agent due to its small diameter and large aspect ratio. The aggregates of MWCNTs, at higher MWCNT content, played a role of α-nucleating agent and the nucleating process of the α-form crystal took place on the surface of the CNT aggregates [8]. At relatively high MWCNTs contents (more than 0.1 wt.%), the width of the melting peak decreased with increasing MWCNTs content and the melting peak temperature increased slightly with increasing MWCNTs content. It indicated that the crystals formed in these iPP/MWCNT composites have a higher degree of crystalline perfection than those in pure iPP. We can conclude that certain content of the individual MWCNTs, namely, certain content of MWCNTs which were dispersed in iPP at the nanoscale, was required to serve as β-nucleating agents.

## WAXD result

To confirm the effect of the MWCNTs on the crystallization of iPP, the crystalline structure of pure iPP and iPP/MWCNT was inspected using WAXD and the corresponding patterns were presented in Fig. 4. Comparison of the WAXD patterns revealed a significant difference between the curve of iPP/MWCNT composite containing 0.1 wt.% MWCNT and the curves of other composites. The characteristic crystalline reflection of α-form iPP at $2\theta$= 13.8° (110), 1.6° (040), 18.3° (130), and 21.5° (111, 131) were observed in the curves of both pure iPP and PP/MWCNT composites with various MWCNT contents. Obviously, the characteristic crystalline reflection of β-form

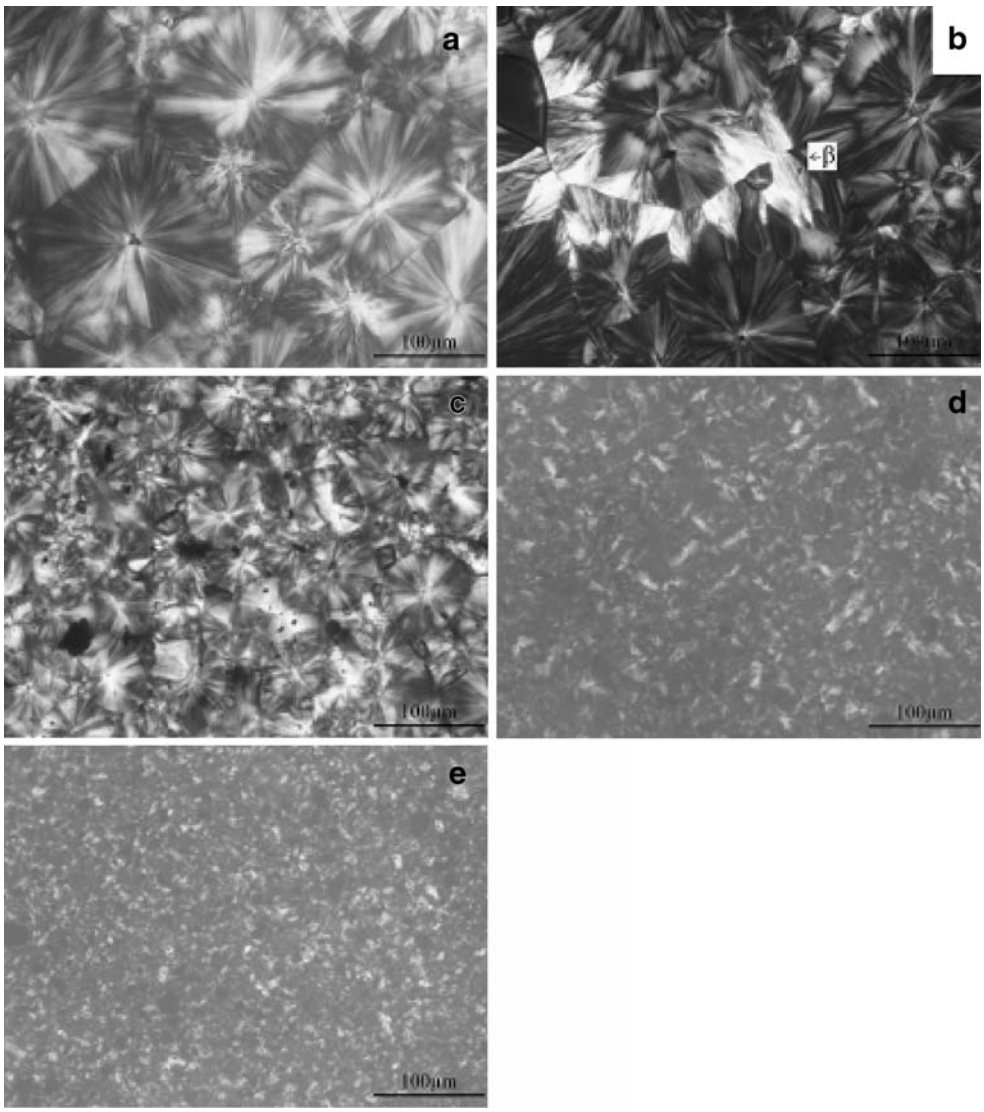


**Fig. 5** PLM micrographs of pure iPP and iPP/MWCNT composites with various MWCNT contents: **a** pure iPP, **b** 0.1 wt.%, **c** 0.5 wt.%, **d** 1 wt.%, and **e** 3 wt.%

iPP at $2\theta=15.9°$ (300) only appeared in the pattern of the iPP/MWCNT composite with a MWCNT content of 0.1 wt.%. The characteristic crystalline reflection of β-phase iPP confirmed the presence of β-crystals in the iPP/MWCNT composite, as shown in the result of DSC previously. It indicated that MWCNTs played as β-nucleating agent on the crystallization of the iPP matrix. The results were in relative disagreement with those proposals that MWCNTs inhibit the formation of the β-iPP crystal.

### Crystalline morphology

In situ PLM observation was carried out to obtain the crystalline morphology of the pure iPP and iPP/MWCNT composites during the nonisothermal crystallization, and the results were shown in Fig. 5. Typical spherulitic morphology was observed in pure iPP and iPP/MWCNT composites with relatively low MWCNTs content (no more than 0.5 wt.%). The spherulite size in the iPP/MWCNT composite with MWCNT content of 0.1 wt.% was almost the same as pure iPP; however, the spherulite size of iPP/MWCNT at 0.5 wt.% MWCNT content was smaller than pure iPP. When the MWCNT concentration reached 1 wt.%, no clear spherulitic morphology was found, and rather distorted crystals were observed in the PLM micrographs. Decrease of the crystal size further indicated that nanotubes acted as nucleating sites for iPP crystallization and increased the crystallization rate of iPP. As shown in Fig. 5b, the bright region between α-spherulites indicated the existence of β-iPP crystal in the iPP/MWCNT composite with 0.1 wt.% MWCNT content. The existence of β-iPP crystal observed in the PLM micrograph confirmed the previous results of DSC and WAXD. Although not shown here, we have also determined the isothermal crystallization behavior of iPP/MWCNT with 0.1 wt.% MWCNTs, at different temperatures. PLM observation showed that the β-crystal iPP existed in the iPP/MWCNT composite with 0.1 wt.% MWCNTs, regardless of nonisothermal crystallization or isothermal crystallization.

## Conclusion

iPP-based composites filled with MWCNTs were prepared by compounding iPP melt with MWCNT aqueous suspension, using a corotating twin-screw extruder, and the morphology and crystallization behavior of the composites were investigated. The SEM micrograph showed that MWCNTs dispersed individually in the iPP matrix at low concentration, though partial MWCNTs aggregated at high content. The presence of MWCNTs, at the concentration of 0.1wt.%, induced the formation of β-crystal iPP due to the low content and individual dispersion state of MWCNTs. In contrast, MWCNTs and MWCNT aggregates acted as α-nucleating agent, at relatively high MWCNT content, and the iPP/MWCNT composites exhibited smaller crystal size and higher degree of crystalline perfection compared with pure iPP. In addition, crystallization temperature and crystallization rate of iPP increased significantly with increasing MWCNT content.

**Acknowledgement** The authors gratefully acknowledge the financial support of this work by the National Natural Science Foundation Commission of China (grant number 10590351).

## References

1. Chang TE, Jensen LR, Kisliuk A, Pipes RB, Pyrz R, Sokolov AP (2005) Polymer 46:439
2. Hou ZC, Wang K, Zhao P, Zhang Q, Ynag CY, Chen DQ, Du RN, Fu Q (2008) Polymer 49:3582
3. Grady BP, Pompeo F, Shambaugh RL, Resasco DE (2002) J Phys Chem B 106:5852
4. Bhattacharyya AR, Sreekumar TV, Liu T, Kumar S, Ericson LM, Hauge RH, Smalley RE (2003) Polymer 44:2373
5. Assouline E, Lusiger A, Barber AH, Cooper CA, Klein E, Wachtel E, Wagner HD (2003) J Polym Sci Part B Polym Phys 41:520
6. Valentini L, Biagiotti J, Kenny JM, Santucci S (2003) Compos Sci Technol 63:1149
7. Seo MK, Lee JR, Park S (2005) J Mater Sci Eng A 404:79
8. Leelapornpisit W, Ton-That M, Perrin-Sarazin F, Cole KC, Denault J, Simard B (2005) J Polym Sci Part B Polym Phys 43:2445
9. Avila-Orta CA, Medellín-Rodríguez FJ, Dávila-Podríguez MV, Aguirre-Figueroa YA, Yoon K, Hsiao BS (2007) J Appl Polym Sci 106:2640
10. Wu DF, Sun YR, Wu L, Zhang M (2008) J Appl Polym Sci 108:1506
11. Lee GW, Jagannathan S, Chae HG, Minus ML, Kumar S (2008) Polymer 49:1831
12. Bikiaris D, Vassiliou A, Chrissafis K, Pataskevopoulos KM, Jannakoudakis A, Docoslis A (2008) Polym Degrad Stab 93:952
13. McIntosh D, Khabashesku VN, Barrera EV (2006) Chem Mater 18:4561
14. McIntosh D, Khabashesku VN, Barrera EV (2007) J Phys Chem C 111:1592
15. Zhou Z, Wang S, Lu L, Zhang Y, Zhang Y (2007) J Polym Sci Part B Polym Phys 45:1616
16. Kelarakis A, Yoon K, Sics I, Somani RH, Chen XM, Hsiao BS, Chu B (2006) J Macromol Sci Part B 45:247
17. Ristolainen N, Vainio U, Paavola S, Torkkeli M, Serimaa R, Seppälä J (2005) J Polym Sci Part B Polym Phys 43:1892
18. Liu ZY, Yu RZ, Yang MB, Feng JM, Yang W, Yin B (2008) Front Chem Eng China 2:115
19. Li W, Liu ZY, Yang MB. J Appl Polym Sci (2008)
20. Li ZF, Luo GH, Zhou WP, Wei F, Xiang R, Liu YP (2006) Nanotechnology 17:3692
21. Marsh DH, Rance GA, Zaka MH, Whitby RJ, Khlobystoy AN (2007) Phys Chem Chem Phys 9:5490
22. Medellín-Rodríguez FJ, Mata-Padilla JM, Hsiao BS, Waldo-Mendoza MA, Ramírez-Vargas E, Sánchez-Valdes S (2007) Polym Eng Sci 47:1889